Hazard Assessment from Storm Tides and Rainfall on a Tidal River Estuary
-
36th IAHR World Congress
28 June – 3 July, 2015, The Hague, the Netherlands

HAZARD ASSESSMENT FROM STORM TIDES AND RAINFALL ON A TIDAL RIVER ESTUARY

P. ORTON[(1)], F. CONTICELLO[(2)], F. CIOFFI[(3)], T. HALL[(4)], N. GEORGAS[(5)], U. LALL[(6)] & A BLUMBERG[(7)]

[(1)] *Stevens Institute of Technology, Hoboken, NJ, United States, philip.orton@stevens.edu*
[(2)] *"La Sapienza" University of Rome, Rome, Italy, federicorosario.conticello@uniroma1.it*
[(3)] *"La Sapienza" University of Rome, Rome, Italy, francesco.cioffi@uniroma1.it*
[(4)] *NASA Goddard Institute for Space Studies, New York, NY, United States, Timothy.M.Hall@nasa.gov*
[(5)] *Stevens Institute of Technology, Hoboken, NJ, United States, ngeorgas@stevens.edu*
[(6)] *Columbia University, New York, NY, United State, e-mail ula2@columbia.edu*
[(7)] *Stevens Institute of Technology, Hoboken, NJ, United States, alan.blumberg@stevens.edu*

ABSTRACT

Here, we report on methods and results for a model-based flood hazard assessment we have conducted for the Hudson River from New York City to Troy/Albany at the head of tide. Our recent work showed that neglecting freshwater flows leads to underestimation of peak water levels at up-river sites and neglecting stratification (typical with two-dimensional modeling) leads to underestimation all along the Hudson. As a result, we use a three-dimensional hydrodynamic model and merge streamflows and storm tides from tropical and extratropical cyclones (TCs, ETCs), as well as wet extratropical cyclone (WETC) floods (e.g. freshets, rain-on-snow events). We validate the modeled flood levels and quantify error with comparisons to 76 historical events.

A Bayesian statistical method is developed for tropical cyclone streamflows using historical data and consisting in the evaluation of (1) the peak discharge and its pdf as a function of TC characteristics, and (2) the temporal trend of the hydrograph as a function of temporal evolution of the cyclone track, its intensity and the response characteristics of the specific basin. A k-nearest-neighbors method is employed to determine the hydrograph shape. Out of sample validation tests demonstrate the effectiveness of the method. Thus, the combined effects of storm surge and runoff produced by tropical cyclones hitting the New York area can be included in flood hazard assessment.

Results for the upper Hudson (Albany) suggest a dominance of WETCs, for the lower Hudson (at New York Harbor) a case where ETCs are dominant for shorter return periods and TCs are more important for longer return periods (over 150 years), and for the middle-Hudson (Poughkeepsie) a mix of all three flood events types is important. However, a possible low-bias for TC flood levels is inferred from a lower importance in the assessment results, versus historical event top-20 lists, and this will be further evaluated as these preliminary methods and results are finalized. Future funded work will quantify the influences of sea level rise and flood adaptation plans (e.g. surge barriers). It would also be valuable to examine how streamflows from tropical cyclones and wet cool-season storms will change, as this factor will dominate at upriver locations.

Keywords: Hudson River, Tropical Cyclones, Hazard Assessment, Hydrodynamic Model, New York

1. INTRODUCTION

As a consequence of two recent tropical cyclone events Irene and Sandy, there has been a regional interest in New York State for developing flood modeling systems useful for a) managing coastal storm emergencies for tropical and extratropical cyclones, b) quantifying flood hazards and how they will evolve with climate change and sea level rise, c) planning coastal protection measures, and d) developing long-term plans for increasing climate change resiliency (e.g., *Gibbs and Holloway*, 2013; *Sobel*, 2014).

A hydrodynamic model was recently applied by Orton et al. (2012) to hindcast flood levels from the August 2011 tropical cyclone Irene and a March 2010 nor'easter that affected low-lying areas around New York Harbor (NYH) and the Hudson River to examine the role of freshwater inputs (among other physical factors) in controlling total water level. One of the most interesting findings was that, even if the storm surge induced by Irene winds, acting against the coastline, was correctly simulated, the errors induced by omitting freshwater inputs from Hudson tributaries and water density variations led to a strong negative bias in flood levels along the Hudson River. This result shows that, in order to develop an effective forecast model of flooding induced by TC in the Hudson, freshwater inputs generated by TC rainfall must be taken into account. Forecast systems, hazard assessments and federal flood mapping typically only evaluate rainfall or surge flooding, and not the merging of the two, and thus risk underestimation of flood hazards (*Orton et al.*, 2012).

The same model is being used to quantify present-day flood hazards for NYH from a combination of tropical cyclones and extratropical cyclones (*Orton et al.*, in preparation). Once the climatology of storms is represented and the flood inundation hazard itself is quantified, this opens to door to adapting the system for forecasting, climate change studies, and adaptation studies (e.g., *Cioffi and Gallerano*, 2003).

Here, we extend this recent hazard assessment work up the extent of the tidal Hudson River and its estuary by merging storm tides and storm-driven streamflows in the model and the hazard assessment. The primary goal of the project is to compute flood hazards for the Hudson River floodplain for today and future decades, including storm surge and rainfall flooding. The study area is the Hudson River from NYH to the Federal Dam at Troy.

2 BACKGROUND: HISTORICAL FLOOD EVENTS AT ALBANY AND BATTERY

The largest flood events from 1931-2012 at NYH and Albany, the southern and northern end of the tidal Hudson River. The historical data utilized in this study is chosen to start at 1931 because that is the first year after the statewide system of reservoirs was completed, most notably the Great Sacandaga Lake and the Conklingville Dam.

Seven of the top-20 events at Battery (NYH; **Figure 1**, left panel) were tropical cyclones (TCs), and the largest was Hurricane Sandy. Extratropical Cyclones (ETCs) cause more frequent flood events, but the historical rankings show an apparent ceiling value of about 2.2 m. The Albany record (**Figure 1**, right panel) shows tropical cyclones (TCs) to have been responsible for four of the top-20 events. A different type of event was defined based on the observation that many events were not TCs but were also not surge-inducing ETC events at the coast (surge was below 1 m). These events typically were rain-on-snow or rain-on-ice events in the cool season (December through May), and account for the other 16 of the top-20 events, and are referred to hereafter as Wet Extratropical Cyclones (WETCs).

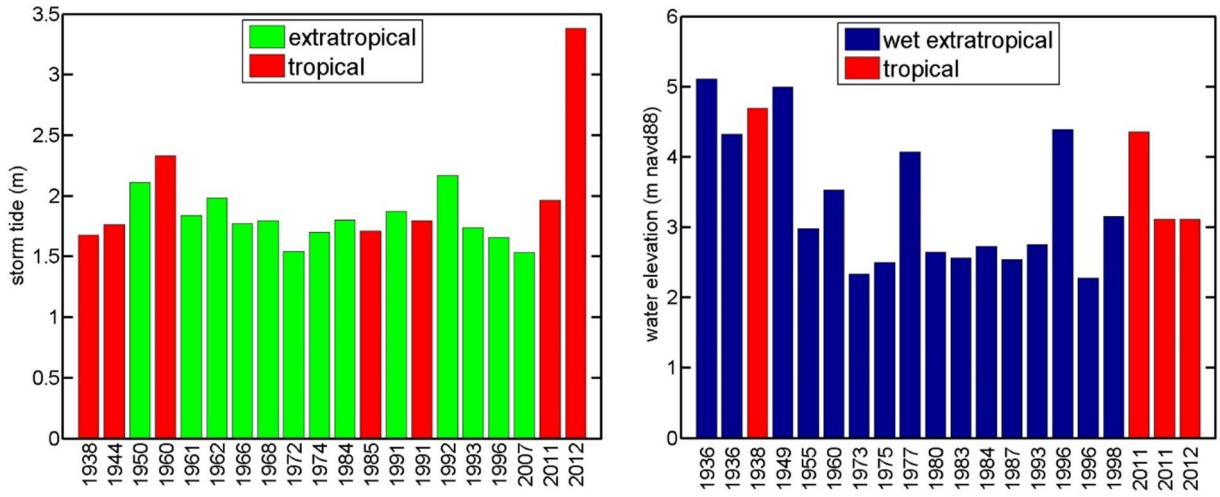

Figure 1. The top-20 highest historical flood events at Battery (New York Harbor, NYH) and Albany from 1931 to 2013 have been a mixture of three different storm types: tropical cyclones (TCs), high-surge extratropical cyclones (ETCs) and high-streamflow "wet extratropicals" (WETCs). Data from (left) NOAA and (right) USGS.

3. METHODS

A detailed operational ocean forecasting system (the New York Harbor Observing and Prediction System, http://stevens.edu/NYHOPS) was leveraged to run three-dimensional ocean simulations for the flood hazard assessment. The general statistical framework for the study is the same framework being used in the separate study of NYH (*Orton et al.*, in preparation), but adding the additional storm type of WETCs (**Figure 1**, right panel). That paper focuses on the oceanic end of the Hudson, where streamflows have a negligible effect on flood risk, so here we also explain methods on streamflows that are not summarized there.

The statistical framework builds an annual rate distribution of water elevations for every location, using model simulations of observed historic events for ETCs and WETCs, and simulated synthetic extreme events for TCs so that rare hurricane events are included in the assessment. Then, the Generalized Extreme Value distribution is fitted to the ETC and WETC rate distributions so that the flood elevations or map contours for a specific return period (from 5-year to 1000-year return periods) can be interpolated (e.g., *FEMA*, 2014). In the case of TCs, the empirical distribution data are smooth enough and capture the long tail of the distribution, so the empirical distribution is used as is (e.g., *FEMA*, 2014). Validation is utilized for each storm type, based on historical storms and measured water levels at Battery, Poughkeepsie and Albany, spaced along the Hudson, and presented in **Section 4.1**.

3.1 Storm types and wind, pressure and tide forcing

A climatology of 533 TCs was built using a statistical-stochastic model of the complete life cycle of North Atlantic (NA) tropical cyclones (*Hall and Yonekura*, 2013). It creates TCs using the statistics of historical North Atlantic TCs (1900 - 2010). A comparison of the modeled and observed historical TC landfall return periods for classes of TC up to Category-3 hurricanes (no Cat-4 TCs have occurred) shows that the TC model is unbiased – the model's return period curve falls inside the 95% confidence range of observed historical return periods (*Orton et al.*, in preparation). We utilize simple parametric equations to represent each storm's wind and pressure forcing for our ocean model – the Holland pressure model (*Holland*, 1980) and SLOSH wind model (*Jelesnianski et al.*, 1992) (**Figure 2**). A set of 30 historical ETCs was utilized to represent the ETC storm tide hazard, and meteorological reanalysis data was available for these storms from a prior FEMA study (*FEMA*, 2014). Detailed summaries of the TC and ETC storm sets, methods for obtaining wind and pressure fields, and other details are given in the separate paper (*Orton et al.*, in preparation).

The WETC storm set was derived by ranking historical streamflows from 1931-2013 at Troy, New York, and choosing the top 35 events that have occurred in "cool season" which is from December through May. Meteorology was not imposed, as the streamflows dominate the water elevations for these storms and high resolution meteorological data for the entire period is not available.

Tides were randomly selected from a time series of tides from 1900-2013, with one simulation with random tide for each TC, one for each WETC, and ten simulations with random tides for each ETC, where tides are a larger proportion of the total water level. Tides were included in the hydrodynamic model, imposed at the edge of the continental shelf as is done with the NYHOPS forecasting system (*Georgas and Blumberg*, 2010).

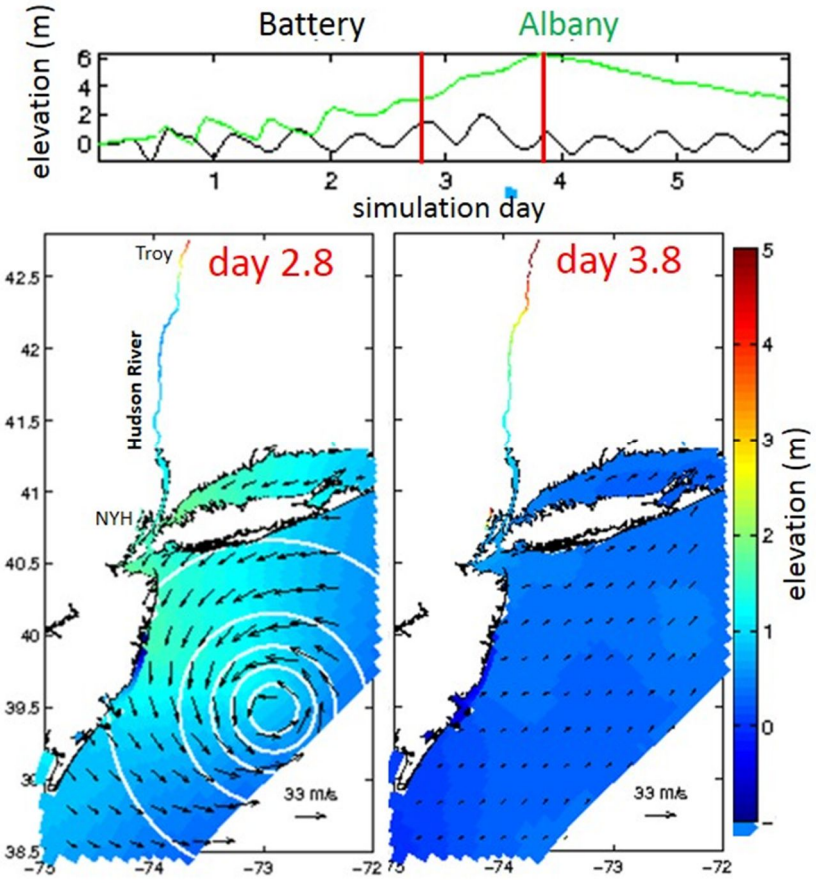

Figure 2. Time progression of a sample synthetic TC flood event (water elevation) with 90th-percentile streamflow.

3.2 HYDRODYNAMIC MODELING

The Stevens ECOM (sECOM) three-dimensional hydrodynamic model (*Blumberg et al.*, 1999; *Georgas and Blumberg*, 2010; *Georgas et al.*, 2014; *Orton et al.*, 2012) has been providing highly accurate storm surge forecasts on its NYHOPS

grid (http://stevens.edu/ NYHOPS) for over a decade, with mean water level errors of 0.10 m since 2007 (*Georgas and Blumberg*, 2010), 0.15 m for Tropical Storm Irene (*Orton et al.*, 2012), and 0.17 m for Hurricane Sandy (*Georgas et al.*, 2014). The NYHOPS grid includes the Mid-Atlantic and Northeastern U.S. coastline from Maryland to Rhode Island (**Figure 2**) and for flood hazard assessment studies is nested inside a NW Atlantic model grid that captures the large-scale influence of winds from Nova Scotia to Cape Hatteras and out to ~2000 km distance offshore. Details of the ocean modeling, including drag coefficient parameterization, wave model coupling, and tide forcing, are all summarized in Orton et al. (*Orton et al.*, in preparation).

3.3 Tributary streamflows

TC streamflow hydrographs were modeled using a statistical Bayesian approach (summarized below) to create streamflows for five tributaries spaced along the Hudson from north-to-south, and across it east-to-west. The chosen tributaries were the Upper Hudson (above lock 1; 11966 km^2), Mohawk (8837 km^2), Wappinger (469 km^2), Rondout (2849 km^2) and Croton (935 km^2). For ETCs and WETCs, we used available historical streamflow data along the Hudson, including the Mohawk, Ft Edward, Hackensack, Passaic, Saddle, Raritan, Manalapan, Esopus, Rondout, Wallkill, Wappinger, Rahway, Croton and Hoosic Rivers. Where only daily data were available (typically prior to 1990), the USGS peak flow estimates for major flood events were inserted into the time series on the day of the peak, to avoid underestimating peak flows during the storms. For all three storm types, ungaged or unmodeled small-to-medium tributaries (the remainder of a total of 52 Hudson River and NYH freshwater inputs to the model) are estimated using the standard NYHOPS system of estimating streamflows based on nearest similar-sized watersheds and scaled by watershed area (*Georgas*, 2010; *Georgas and Blumberg*, 2010).

3.4 Statistical Bayesian approach to translate TC attributes to streamflows

Many prior studies have targeted improvements in rainfall forecasting, but this is just a part of the problem of the quantification of the spatial structure of flooding over a region, since simulated rainfall fields have to be combined with hydrologic and hydraulic models of runoff production and transport through the drainage network. This approach requires implementation of hydrologic models for flood hazard characterization, which can be difficult to apply, especially across large regions (*Villarini et al.*, 2014) or where rainfall data are scarce. An alternative is to develop statistical data-driven approaches based on discharge observations from streamflow measurements (*Villarini et al.*, 2014).

Here, a statistical model is constructed that utilizes the parametric attributes of a TC that has been simulated by the TC model (*Hall and Yonekura*, 2013) to create streamflow hydrographs at specific points of the tributaries of the Hudson River. A hydrograph is identified by the following variables: (a) the initial discharge Q_{init}, (b) the peak discharge, (c) the timing of the peak discharge relative to TC timing, and (d) the hydrograph shape.

A Bayesian Simultaneous Quantile Regression approach (*Reich and Smith*, 2013) is used to translate the TC attributes (storm track, sea surface temperature - SST, maximum wind speed) into discharge peaks; a multivariate normal distribution is used to determine the time shift associated with the TC track; and lastly a KNN method is employed to determine the hydrograph shape. To construct the statistical model we used HURDAT 2 data (http://www.aoml.noaa.gov/hrd/hurdat/Data_Storm.html) with climatological along-track SST data for 1938 to 2012 TCs. For each 6 hour step the dataset provides longitude and latitude of the TC low pressure center and the maximum sustained wind speed, among other variables. From the dataset we identified 103 hurricanes whose track passed within a radial distance of 400 km from NYH. Beyond this distance, the TC rainfall contribution drops significantly and can be assumed to be negligible (*Frank*, 1977; *Rodgers et al.*, 1994). Flow rate data are taken from USGS gauges, and only the streamflow data associated with TCs in the HURDAT dataset were used to build the statistical model.

Discharge peak evaluation

Empirical analysis of data, together with inferences deduced by the physical mechanisms of genesis, development and lysis of TCs (*Emanuel*, 1991), suggest that the peak streamflows for a TC are higher if the track is closer to a river basin and if the energy content of the cyclone is higher. Coarsely, we can say that TC energy grows with the time a TC spends over the ocean, and TC energy is proportional to SST along the storm track. Alternatively, if part of the storm track is over land, the peak streamflows are lower, and this decrease is related to the total time the TC stays over land. Here, we assume TC energy is related to the integral of SST along the time interval in which the track is over the ocean, from the time of generation until the time of minimum distance from the center of the river basin, D.

Thus, we can identify a set of TC variables significantly affecting the peak discharge:

a) the minimum distance *D* from the TC track to the center of the basin
b) the maximum sustained wind speed V_{max} at the time the TC reaches the minimum distance
c) the integral of SST along the time interval in which the track is over the ocean, from the time of generation until the time of minimum distance, *ISST*;
d) the total time over land along the TC track, “ground permanence” (*GP*).

The variables describing TC attributes are combined in a unique variable *X* by the following relation:

$$X = \log \frac{w_1 ISST^{w_2} + w_3 V_{\max}{}^{w_4} + w_5 Q_{init}{}^{w_6}}{w_7 D^{w_8} + w_9 GP^{w_{10}}} \qquad [1]$$

In the denominator of Eq (1) there are the quantities whose increase produces a decrease in peak discharge, and in the numerator, the contrary. Thus, increases in *X* lead to increases in the peak discharge. A Bayesian Simultaneous Quantile Regression (*Reich and Smith*, 2013) is applied to find the relationship between the covariate *X* and the response $y = \ln Q$ (being *Q* the peak discharge). An MCMC algorithm (*Besag et al.*, 1995; *Gelfand and Smith*, 1990; *Tanner and Wong*, 1987) is then applied to identify the parameters (w_i) of the Bayesian model. The described approach does not determine a single value of peak discharge but the PDF of peak discharge as a function of the TC variables previously combined in the covariate *X*.

The results of the Bayesian Simultaneous Quantile Regression for the Mohawk River are shown in **Figure 3**. In the left panel is the relationship between parameter *X* (normalized between -1 and 1) and peak discharge for the regression interpolation for the 10th (black), 50th (red) and 90th (green) percentile values of peak discharge. In the right panel of **Figure 3** are the probability distributions peak discharge as functions of the assigned values of X, where X = -0.8 (black), X = 0 (red) and X = 0.8 (green). The left panel shows a positive correlation between *X* and the peak discharge for all quantile levels; so the variable *X* appears to be a good predictor for peak discharge in the Mohawk. Similar results are found for the other four river basins. Furthermore, the highest quantile has a steeper slope. Therefore, it appears that the combined variable X is a stronger predictor of extreme peak discharge events than the median and other quantile levels.

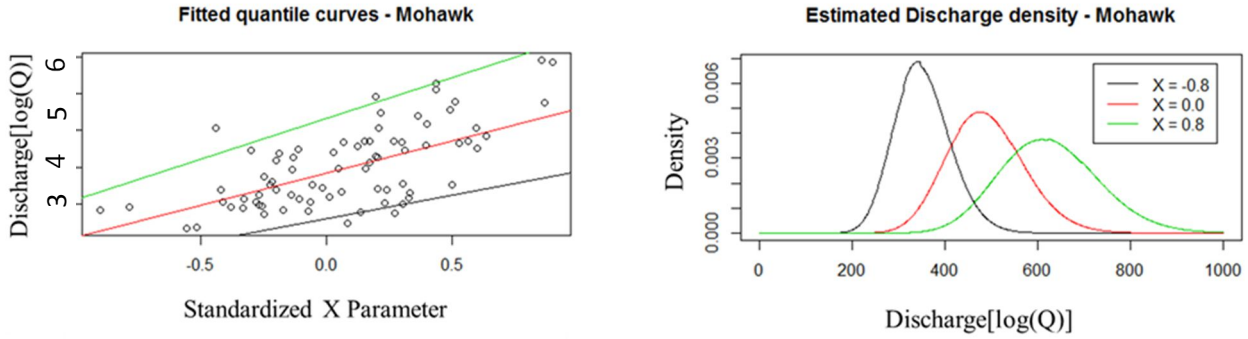

Figure 3. Bayesian Quantile Regression Results. On the left of the figure there are three fitted quantile curves for 90th (green), 50th (red), and 10th (black) percentile. On the right there are three PDFs in function of three different X values: 0.8 (green), 0.0 (red) and -0.8 (black).

Hydrograph shape and timing of peak discharge

We assume that the hydrograph could be divided into two branches, an ascending branch with flow rate that increases till the peak, and a decreasing branch. The former depends on both the TC track and basin characteristics, while the latter mainly depends on basin characteristics. Then, the normalized flow rate vector and distance vector for each historical cyclone are calculated as:

$$\tilde{q}_{hist,k,j} = \frac{q_{hist,k,j}}{\max(q_{hist,k,j})} \qquad [2]$$

$$\tilde{r}_{hist,k,j} = \frac{r_{hist,k,j} - \min(r_{hist,k,j})}{\max(r_{hist,k,j}) - \min(r_{hist,k,j})} \qquad [3]$$

Here, *k=(1,T)* is the time step and *j=(1,N)* is the *j*th cyclone.

The steps of the procedure for the calculation of hydrograph shape are the following:

1) a conditional distribution of the peak discharge $q_{peaksim}$ is generated for each basin by Bayesian Quantile Regression as a function of the TC attributes and its track $r_{sim}(t)$;
2) a peak discharge $q_{peaksim}$ - having a pre-fixed percentile - from that conditional distribution is sampled;
3) from the dataset of historical peak discharges, *Nc* nearest neighbors hydrographs $\tilde{q}_{hist,k,j}$, whose peak discharge is closer to $q_{peaksim}$, are identified;

4) the temporal axes of the *Nc* normalized historical cyclone tracks $\tilde{r}_{hist,k,j}$ and hydrographs $\tilde{q}_{hist,k,j}$ are shifted to have a common origin in correspondence of the peak discharge ;
5) the normalized ascending branch of the hydrograph corresponding to $q_{peaksim}$ is assumed equal to the trend of the normalized historical hydrograph $\tilde{q}_{hist,k,j}$ having the peak discharge q_{hist} closer to $q_{peaksim}$;
6) the normalized decreasing branch of the hydrograph after the peak - which depends mainly on the characteristics of the basin - is represented by a negative exponential function whose parameters are obtained by a best fitting of the normalized hydrographs of the *Nc* nearest neighbors;

The steps for the calculation of the peak discharge time shift are the following (noting "cor" is correlation):

1) the 25th, 50th, and 75th percentiles of historical peak flows q_{hist} are calculated and four peak discharge classes are defined: q_{hist} <25th, 25th<= q_{hist} <=50th, 50th<= q_{hist} <=75th, and q_{hist} >75th;
2) the class of peak discharge $q_{peaksim}$ is identified as well as the TC normalized tracks and corresponding normalized hydrographs belonging at that class;
3) assuming that $\tilde{q}_{hist,k,j}, \tilde{r}_{hist,k,j}$ are normally distributed with respectively mean μ and υ, standard deviation σ and τ, and cor ($\tilde{q}_{hist,k,j}, \tilde{r}_{hist,k,j}$)=$\rho$, a joint probability function can be identified as:

$$f\left(\tilde{q}_{sim,k}, \tilde{r}_{sim.k}\right) = \frac{1}{2\pi\sigma\tau\sqrt{1-\rho^2}} e^{\left\{-\frac{1}{2(1-\rho^2)}\left[\frac{(\tilde{q}_{sim,k}-\mu)^2}{\sigma^2} - 2\rho\frac{(\tilde{q}_{sim,k}-\mu)(\tilde{r}_{sim,k}-\upsilon)}{\sigma\tau} + \frac{(\tilde{r}_{sim,k}-\upsilon)^2}{\tau^2}\right]\right\}} \quad [4]$$

For a known sequence of $\tilde{r}_{sim.k}$, at each time step the joint probability distribution of $\tilde{q}_{hist,k,j}$ can be calculated and the time step *k* corresponding to max($\tilde{q}_{hist,k,j}$) obtained.

A validation test of the above cited methods is shown in **Figure 4** for the Mohawk Watershed, with the observed (green) and simulated (red) hydrographs for TCs that have produced from medium (left panel) to high (right panel) peak discharge are shown. In most of the cases and across a wide range of TC characteristics, the model captures both the correct temporal trend of the hydrograph as a function of the position in time of the TC center, and the shape of hydrograph, that is representative of the flood volume during the event. The latter quantity, together with the peak discharge plays and important role on the flooding phenomena along the Hudson River downstream of the tributary inlets.

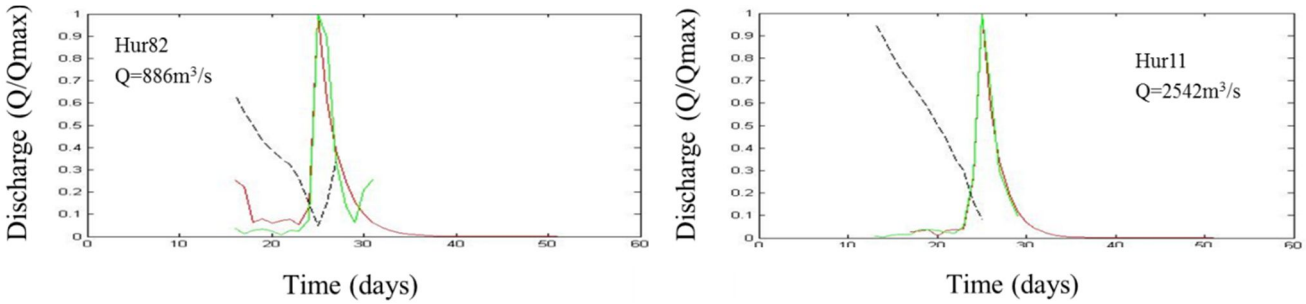

Figure 4. Results for the shape model of several discharge rate at Mohawk River, for historical cases of medium (left) and high (right) TC discharge. In green is represented the observation and in red the simulation. The black dashed line is the distance of the TC from the center of the basin. Discharge is normalized by the peak during the each event, and distance is normalized by the maximum distance from the watershed.

Application of model to hydrodynamic modeling of TCs

In order to carry out a risk analysis of the flooding phenomena in NYH and along the Hudson River, we used the model to generate a large number of synthetic hydrographs to accompany the TC storm set. As an example, the synthetic series of hydrographs related to the 533 TCs and to Mohawk River is shown in **Figure 5**.

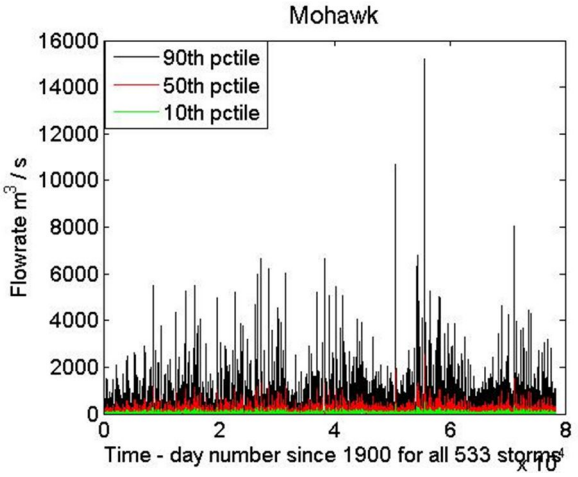

Figure 5. The complete time series of synthetic Mohawk River (at Cohoes) discharge for 533 synthetic storms, shown back-to-back, with flow rates for each percentile

Three model runs are performed for each TC, each with a different percentile streamflow peak (10th, 50th and 90th percentile). For scaling the annual rates to enter the modeled flood elevation results into the TC annual rate distributions, we consider these as mean values of flows belonging to a three classes of probability (100-80, 80-20, 20-0). As a result, the storm annual rates are scaled by 0.2, 0.6 and 0.2 respectively for the three classes. This should be a good approximation to the complete spectrum of streamflows for each TC, balancing computational time (3 model runs per storm representing the range of possible TC streamflows) against possible error, and is similar to our representation of other variables with three classes (e.g. landfall angle, storm size, storm speed). The total number of storms then is multiplied by 3, equaling a total of 1599 TCs.

4.0 RESULTS

4.1 Storm tide modeling validations

Comparisons of historical observed and modeled temporal maximum water levels (storm tides) are shown for each storm type in **Figure 6**. A set of 11 historical TC events from 1821 to present, and the sets of 30 historical ETCs and 35 historical WETCs were modeled with historical tides. For TCs, model mean bias is below 1 cm and root-mean-square error (RMSE) is 0.25 m. Hurricane Sandy is overestimated by 0.55 m, whereas a few other intense storms (e.g. 1960, Donna; 1821, the Norfolk and Long Island Hurricane) were underestimated. A majority of the storms is simulated very accurately, within 0.20 m (1893, 1954, 1976, 1985, 1999, and 2011). Details of the observational data and sources of parametric TC meteorological data for the Holland and SLOSH models are discussed in Orton et al (*Orton et al.*, in preparation). The ETC validation has a storm tide mean bias of -0.03 m and an RMSE of 0.19 m, though the 1950 ETC had its wind speed multiplied by 0.82 due to it being the most important (highest surge) event and having a very poor validation result otherwise (*Orton et al.*, in preparation). The validation for the WETCs shows a mean bias of +0.06 m and RMSE of 0.39 m.

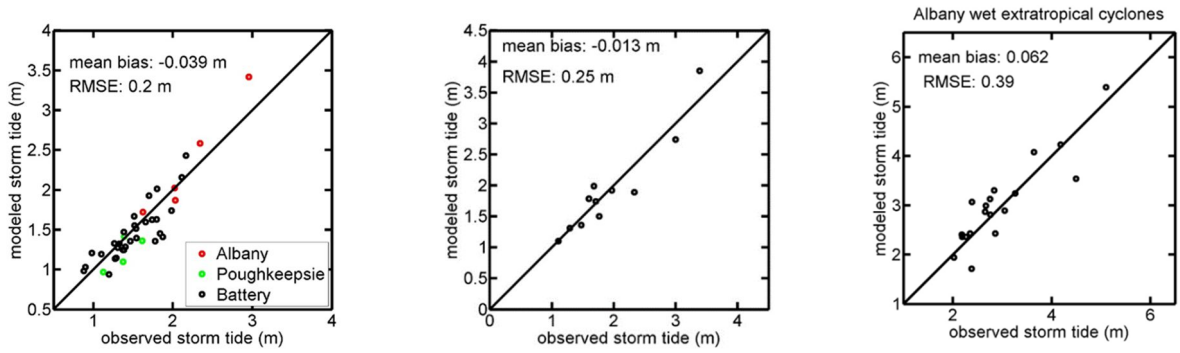

Figure 6. Model-observation comparisons for the peak water levels (storm tide) for historical TCs, ETCs, and WETCs (e.g. rain-on-snow event). The left panel is for ETCs, and shows data for Albany, Battery and Poughkeepsie, the center panel shows TCs and data at Battery, and the right panel shows WETCs with data at Albany.

4.2 Statistical distributions and flood exceedance curves

Annual rate distributions were constructed form model results at each model grid cell for TCs, ETCs, and WETCs (**Figure 7**). These were utilized to compute flood exceedance curves, and are shown for three along-Hudson sites in **Figure 8**. Exceedance probabilities for each type are merged to create the combined flood exceedance curves, representing the return period for any type of flooding along the Hudson, and similar data are available for all grid cells within the model domain. The curves show that Albany results are dominated by WETCs. Poughkeepsie results show a flood hazard that is a mixture of all three storm types. Battery results (right) show a dominance of ETCs and TCs, with cross-over at the 150-year return period.

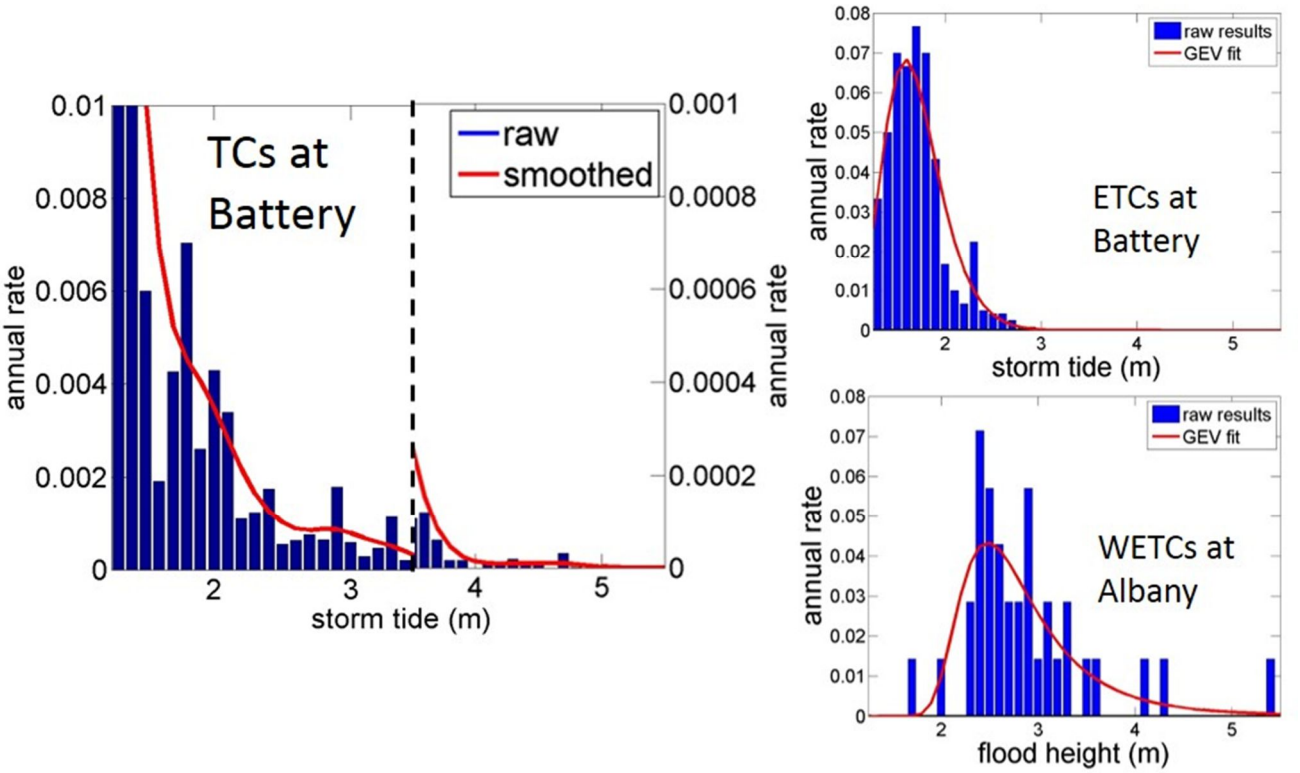

Figure 7. Annual rate distributions for TCs, ETCs and WETCs at Battery or Albany. For TCs, the right hand side has its y-axis zoomed by a factor of 10.

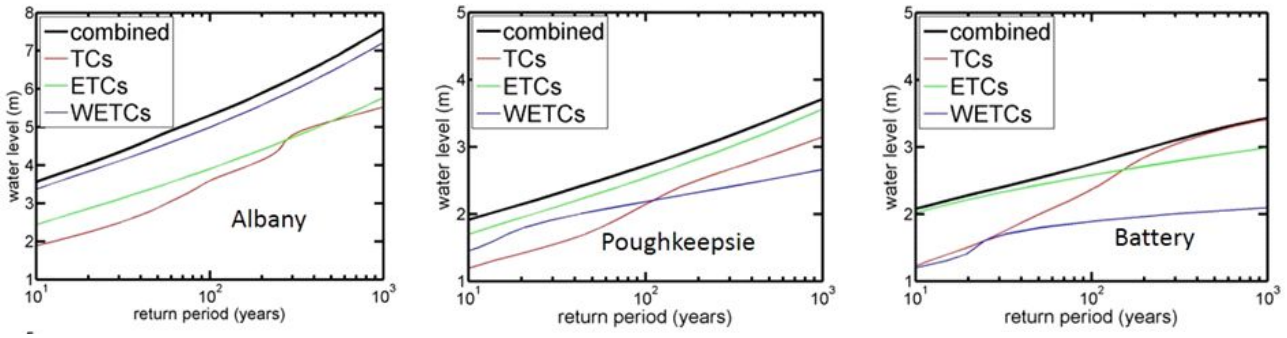

Figure 8. Flood exceedance curves at each location are a mixture of event types. Black lines show the combined flood hazard assessment, merging exceedance probabilities from TCs, ETCs, and WETCs. Water levels in this final figure are adjusted to be relative to Battery mean sea level, a datum 0.06 m below NAVD88.

5. DISCUSSION AND CONCLUSIONS

Prior to interpreting the results in **Figure 7** as telling us what types of storm actually dominate at sites along the Hudson, they should considered alongside historical observations of the top-20 events, shown in **Figure 1**. For Albany, the assessment results suggest a dominance of WETCs, but the historical events suggest that TCs are also important. This may reflect a bias in the study, and that will need to be further evaluated. Alternatively, the result could reflect that the 1931-2013 period was not reflective of the actual flood risks from TCs versus WETCs. A second draft of results is now being produced, and this matter is being evaluated. One possible explanation for underestimating the flood risk at Albany would be the omission of TCs that follow an over-land route far to the west of NYH. These are not represented in the storm set, as it was focused on NYH storm tide events (*Orton et al.*, in preparation). One of the four TCs in the top-20 list (**Figure 1**) did not pass the landfall gates that are represented in the storm set – the remnant extratropical storm that formed from Hurricane Lee in 2011, so the impact of these events will need to be quantified, perhaps by broadening the WETC storm set to include hurricane season events.

For the Battery, our assessment results show ETCs and TCs are both important. The results suggest ETCs dominate shorter return periods, and TCs are more important for the longer return periods, with a cross-over point a return period of about 150 years. The historical events show ETCs to account for the most top-20 events, but TCs to account for the top two. However, it is difficult to determine the importance of TCs to the 100-year flood from such a short record, particularly given the extreme outlier of Hurricane Sandy's water level. Poughkeepsie's flood exceedance curve shows a mix of all three storm types, further validating the study's approach of considering all three types of storms.

Other recent studies have evaluated the flood hazard for NYH, and have found widely diverging exceedance curves (*Orton et al.*, in preparation). The 100-year storm tide at NYH has had estimates ranging from 2.0 m (*Lin et al.*, 2012) to 3.5 m (*FEMA*, 2014). Our result of 2.7 m falls between these studies and is within the 90% confidence range of an estimated exceedance curve based on historical data (*Orton et al.*, in preparation). At Albany, FEMA's flood maps show a 100-year flood elevation of 6.2 m, about 0.9 m higher than our result.

The Bayesian modeling of TC streamflows have been highly useful in this study, whereas TC rainfall simulation and detailed hydrological modeling proved to be too time-intensive to set up, and may not have given as useful results. The validation tests have demonstrated the capability of the Bayesian model, in most of the cases and for very different TC characteristics, to capture both the shape of hydrograph and the correct temporal trend of the hydrograph as a function of the position in time of the TC center, reasonably representing the total flood volume during the event. The peak flood timing, together with the peak discharge, plays and important role on the flooding phenomena along the Hudson River downstream of the tributary inlets. Benefits of using the statistical streamflow model included the simplicity of using observed streamflow records, and the model output in terms of percentiles of streamflow. Possible shortcomings of the proposed method is that it requires a consistent, numerous streamflow and TC dataset to identify the model parameters. If this requirement is satisfied, it can be applied to other hydrologic systems.

This hazard assessment approach holds promise for many coastal regions where storm surge and fluvial flooding merge, avoiding the possible low-bias caused by evaluating each separately based on an assumption of statistical independence. Other noteworthy tidal river systems with mixed surge and rain flood hazards exist, including river estuaries of North Carolina (*Dresback et al.*, 2013), Texas (*Ray et al.*, 2011), Chesapeake Bay (*Loftis et al.*, 2014), and other global river estuaries (*Chen et al.*, 2012), and these methods may also prove useful for hazard and risk assessment in these locations.

The assessment is useful for understanding flood risk, improving disaster management through extreme flood scenarios, studying how climate change will impact future flooding, and quantitatively evaluating flood adaptation measures. One example of a flood adaptation measure that could uniquely be evaluated using this assessment is a cross-harbor storm surge barrier at NYH, which has been considered as a possible solution for the entire harbor region. The storm set gives a wide range of flood events from both storm tides and rainfall, so that the barrier's influence on both types of flooding could be evaluated, including the potential for trapping of rainfall flooding and resulting duration it can be closed.

The results of the study are being used to map flood zones along the Hudson River, for 5-year to 1000-year floods as part of an online mapping tool that includes damage assessments for different flood events and sea level rise scenarios. The tool will enable planners and populations in the region to better understand and plan for possible flood events and worsening future flooding. Future funded work will quantify the influences of sea level rise and flood adaptation plans (e.g. surge barriers). It would also be valuable to examine how streamflows from tropical cyclones and wet cool-season storms will change, as heavy rainfall episodes have been increasing over the U.S. Northeast (*Peterson et al.*, 2013), and a continued increase is projected with climate change (e.g., *New York City Panel on Climate Change*, 2013). Due to the dominance of streamflow over storm surge at upriver locations like Albany, this factor could control the future evolution of flood hazards in these areas.

ACKNOWLEDGMENTS

Research funded by New York State Energy Research and Development Authority (NYSERDA; Blumberg, PI), the NASA Centers call for support of the National Climate Assessment (Hall, PI), the NOAA-RISA project "Consortium for Climate Risk in the Urban Northeast" (Rosenzweig, PI) and a NASA Interdisciplinary Research in Earth Science project (Kushnir, PI). Modeling was made possible by a grant of computer time from the City University of New York High Performance Computing Center under NSF Grants CNS-0855217, CNS-0958379 and ACI-1126113.

REFERENCES

Besag, J., P. Green, D. Higdon, and K. Mengersen (1995). Bayesian computation and stochastic systems. *Statistical science*, 3-41.

Blumberg, A. F., L. A. Khan, and J. St John (1999). Three-dimensional hydrodynamic model of New York Harbor region. *J. Hydraul. Engin.*, *125*(8), 799-816.

Chen, W.-B., W.-C. Liu, and M.-H. Hsu (2012). Comparison of ANN approach with 2D and 3D hydrodynamic models for simulating estuary water stage. *Advances in Engineering Software*, *45*(1), 69-79.

Cioffi, F., and F. Gallerano (2003). A two-dimensional self-adaptive hydrodynamic scheme for the assessment of the effects of structures on flooding phenomena in river basins. *River Research and Applications*, *19*(1), 1-26.

Dresback, K. M., et al. (2013). Skill assessment of a real-time forecast system utilizing a coupled hydrologic and coastal hydrodynamic model during Hurricane Irene (2011). *Cont. Shelf Res.*, *71*, 78-94.

Emanuel, K. A. (1991). The theory of hurricanes. *Annual Review of Fluid Mechanics*, *23*(1), 179-196.

FEMA (2014). Region II Coastal Storm Surge Study: Overview, 15 pp, Federal Emergency Management Agency, Washington, DC.

Frank, W. M. (1977). The structure and energetics of the tropical cyclone II. Dynamics and energetics. *Monthly Weather Review*, *105*(9), 1136-1150.

Gelfand, A. E., and A. F. Smith (1990). Sampling-based approaches to calculating marginal densities. *Journal of the American statistical association*, *85*(410), 398-409.

Georgas, N. (2010). Establishing confidence in marine forecast systems: The design of a high fidelity marine forecast model for the NY/NJ harbor estuary and its adjoining coastal waters, 272 pp, Stevens Institute of Technology.

Georgas, N., and A. F. Blumberg (2010). Establishing Confidence in Marine Forecast Systems: The Design and Skill Assessment of the New York Harbor Observation and Prediction System, Version 3 (NYHOPS v3). Paper presented at Eleventh International Conference in Estuarine and Coastal Modeling (ECM11), ASCE, Seattle.

Georgas, N., P. Orton, A. Blumberg, L. Cohen, D. Zarrilli, and L. Yin (2014). The Impact of Tidal Phase on Hurricane Sandy's Flooding Around New York City and Long Island Sound. *Journal of Extreme Events*, DOI: 10.1142/S2345737614500067.

Gibbs, L., and C. Holloway (2013). Hurricane Sandy After Action, Reports And Recommendations To Mayor Michael R. *Bloomberg. New York, NY: Deputy Mayors of NYC*.

Hall, T., and E. Yonekura (2013). North American tropical cyclone landfall and SST: A statistical model study. *J. Clim.*, *26*(21), 8422-8439.

Holland, G. J. (1980). An analytic model of the wind and pressure profiles in hurricanes. *Monthly Weather Review*, *108*(8), 1212-1218.

Jelesnianski, C., J. Chen, W. Shaffer, U. S. N. Oceanic, A. Administration, and U. S. N. W. Service (1992). *SLOSH: Sea, lake, and overland surges from hurricanes*, US Dept. of Commerce, National Oceanic and Atmospheric Administration, National Weather Service.

Lin, N., K. Emanuel, M. Oppenheimer, and E. Vanmarcke (2012). Physically based assessment of hurricane surge threat under climate change. *Nature Climate Change*.

Loftis, J. D., H. V. Wang, R. J. DeYoung, and W. B. Ball (2014). Integrating Lidar Data into a High-Resolution Topobathymetric DEM for Use with Sub-Grid Inundation Modeling at Langley Research Center. *Journal of Coastal Research*.

New York City Panel on Climate Change (2013). Climate risk information 2013: Observations, climate change projections, and maps, Prepared for use by the City of New York Special Initiative on Rebuliding and Resiliency, New York, NY.

Orton, P., N. Georgas, A. Blumberg, and J. Pullen (2012). Detailed Modeling of Recent Severe Storm Tides in Estuaries of the New York City Region. *J. Geophys. Res.*, *117*, C09030, DOI: 10.1029/2012JC008220.

Orton, P. M., T. M. Hall, S. Talke, N. Georgas, A. F. Blumberg, and S. Vinogradov (in preparation). A Detailed, Validated Flood Hazard Assessment for New York Harbor. *J. Geophys. Res.*

Peterson, T. C., et al. (2013). Monitoring and understanding changes in heat waves, cold waves, floods, and droughts in the United States: State of knowledge. *Bull. Amer. Meteorol. Soc.*, *94*(6), 821-834.

Ray, T., E. Stepinski, A. Sebastian, and P. B. Bedient (2011). Dynamic modeling of storm surge and inland flooding in a Texas coastal floodplain. *J. Hydraul. Engin.*, *137*(10), 1103-1110.

Reich, B. J., and L. B. Smith (2013). Bayesian quantile regression for censored data. *Biometrics*, *69*(3), 651-660.

Rodgers, E. B., J.-J. Baik, and H. F. Pierce (1994). The environmental influence on tropical cyclone precipitation. *Journal of Applied Meteorology*, *33*(5), 573-593.

Sobel, A. H. (2014). *Storm Surge: Hurricane Sandy, Our Warming Planet, and the Extreme Weather of the Past and Future*, Harper Wave.

Tanner, M. A., and W. H. Wong (1987). The calculation of posterior distributions by data augmentation. *Journal of the American statistical Association*, *82*(398), 528-540.

Villarini, G., R. Goska, J. A. Smith, and G. A. Vecchi (2014). North Atlantic tropical cyclones and US flooding. *Bull. Amer. Meteorol. Soc.*, *95*(9), 1381-1388.